PAPER

Check for updates

An intramolecular relay catalysis strategy for Knoevenagel condensation and 1,3-dipolar cycloaddition domino reactions†

Xiaofeng Yuan,[a] Zijuan Wang,[a] Qiang Zhang [ID][b] and Jun Luo [ID] *[a]

A relay catalysis strategy was established by using a bifunctional catalyst which was prepared by immobilization of organic chains containing secondary amine and Cu(II) complex onto silica-coated nano-Fe$_3$O$_4$. The simply prepared nanoparticles acted as efficient, intramolecular relays and magnetically recyclable base-metal bifunctional catalysts for Knoevenagel condensation and 1,3-dipolar cycloaddition domino reactions to prepare 5-substituted 1H-tetrazoles with excellent yields.

Introduction

Multifunctional catalysts for one-pot multistep reactions have attracted much attention recently owing to their high efficiency.[1–12] Bifunctional catalysts with different catalytic centers on separate or the same supports are the dominant targets in this field.[13–33] For example, Shylesh et al. used organic amines and sulfonic acid bifunctionalized porous organosilicas in one-pot deacetalization–nitroaldol cascade reactions.[16] Shiju et al. prepared an efficient and robust bifunctional acid–base solid catalyst and evaluated the catalytic activities in deprotection–Henry domino reactions and deprotection–aldol reactions.[17] Huang et al. prepared a bifunctional mesoporous silica nanoparticle with sulfonic acid moiety on its internal surface and organic amine moiety on its external surface and applied it in deacetalization–Henry cascade reactions.[28] To sum up, the reported bifunctional supported catalysts were constructed by mainly two strategies: parallel immobilization of different catalytic moieties on the surface of the same support (Fig. 1(a)) or separate immobilization of different catalytic moieties on the internal and external surface respectively (Fig. 1(b)). The two design ideas are smart and attractive. However, for domino reactions, the mass transfer of intermediate products between two catalytic centers still needs time and energy. So, how can we make the transfer procedure more efficient? With this question in mind, we put forward a new strategy by sequentially connecting different catalytic moieties on the same organic chain and immobilizing it on the surface of one support (Fig. 1(c)).

Magnetic nanoparticles (MNPs) are attractive catalyst supports because they have advantages of excellent dispersion, easy separation and high compatibility with numerous kinds of catalysts.[34–42] Among them, silica coated MNPs attract increasing interests because they have a considerable amount of derivable hydroxyl groups and can be easily functionalized by catalyst-containing organosilicate esters.[29,43–56] Our previous work speculated that the reactants would be adsorbed on the surface of the nano-support, so the local concentration of reactants around the catalytic sites would increase and then effectively elevate the reaction rate.[48]

The new relay catalysis using easily recyclable bifunctional nano-catalysts is illustrated in Fig. 2.

5-Substituted 1H-tetrazoles have extensive applications in chemistry.[57–65] The conventional synthesis of these compounds is [2 + 3] cycloaddition of nitriles with azide salts.[66,67] A variety of catalysts for this transformation have been reported.[68–81] However, the reported methods have one or more drawbacks such as use of highly toxic reagents, high cost, elevated reaction temperature, long reaction time or unsatisfactory recovery of catalyst. Therefore, the demand of efficient, economical and greener method for the preparation of 5-substituted 1H-tetrazoles is still demanded.
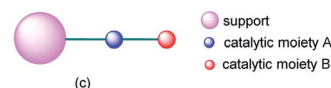
[a]School of Chemical Engineering, Nanjing University of Science and Technology, Nanjing 210094, China. E-mail: luojun@njust.edu.cn

[b]Jiangsu Key Laboratory of Environmental Functional Materials, School of Chemistry, Biology and Material Engineering, Suzhou University of Science and Technology, Suzhou 215009, China

Fig. 1 Strategies of nanoparticle-supported bifunctional catalysts.
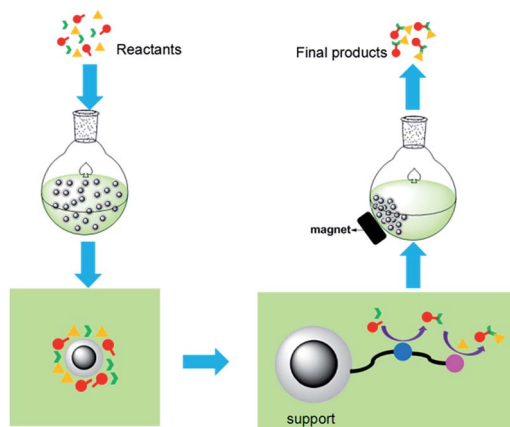
Fig. 2 Ideal relay catalysis for domino reactions.

Herein, we reported a new relay catalysis system involving the establishment of a secondary amine/Cu(II) bifunctional magnetic nanoparticle (NH–Cu(II)@MNP) characteristic of sequentially connecting secondary amine and copper(II) complex on the same organic chain, and application of it as efficient, intramolecular relay and magnetically recyclable bifunctional nano-catalyst in the one-pot synthesis of 5-substituted 1H-tetrazoles through Knoevenagel condensation and 1,3-dipolar cycloaddition domino reactions.

Results and discussion

The procedure for the preparation of the nano-Fe_3O_4 supported secondary amine/Cu(II) bifunctional catalyst (NH–Cu(II)@MNP) is shown in Scheme 1. The support Fe_3O_4@SiO_2 were prepared according to our previous work.[48] Then [3-(2-aminoethyl)ami-nopropyl]triethoxysilane was introduced onto Fe_3O_4@SiO_2 through a condensation reaction. After that, the secondary amine functionalized precursor NH-L@MNP (**2**) was prepared by a condensation reaction of compound **1** with pyridine-2-carbaldehyde. Meanwhile, the loading amount of the organic motif was determined to be 0.20 mmol g^{-1} by elemental analysis, which was also in accordance with thermogravimetric (TG) test. Ultimately, **2** was coordinated with $Cu(OAc)_2$ in acetone at room temperature for 24 h to give the target catalyst **3**.
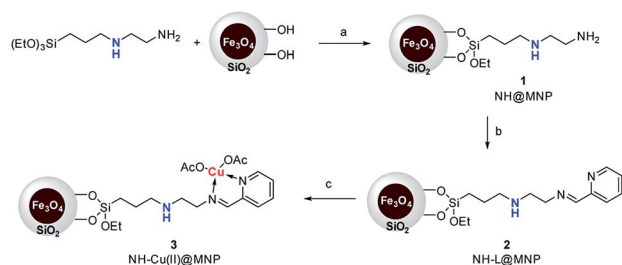
The Fourier transform infrared (FT-IR) spectra of Fe_3O_4@SiO_2 and catalyst **3** are demonstrated in Fig. 3. The spectrum of Fe_3O_4@SiO_2 shows a moderate peak at 586 cm^{-1} (Fe–O vibration), a strong peak at 1087 cm^{-1} (Si–O–Si stretching vibration), a broad weak peak around 3263 cm^{-1} (O–H stretching vibration) and a weak peak at 1602 cm^{-1} (adsorbed water). All of these characteristic signals are observed in the spectrum of **3**. Moreover, **3** shows typical bands at 1597 cm^{-1} (C=N vibration) and 1446 cm^{-1} (C=C vibration of aryl ring). These results indicate that organic moiety was successfully immobilized onto Fe_3O_4@SiO_2.

Fig. 4 shows the X-ray diffraction (XRD) patterns of Fe_3O_4@SiO_2 and **3**. Both samples have the diffraction peaks on the standard Fe_3O_4 sample (Fig. 4(a), JCPDS file no. 19-0629). The broad peak of $2\theta = 20–30°$ belongs to silica layer. The pattern of **3** (Fig. 4(b)) is similar to that of Fe_3O_4@SiO_2. But the intensity becomes weak in Fig. 4(b), indicating that the structure of Fe_3O_4@SiO_2 remains unchanged after being functionalized. The average crystal size of the Fe_3O_4 cores is about 11.4 nm according to the Scherrer formula.

The transmission electron microscope (TEM) images of Fe_3O_4@SiO_2 and **3** were recorded (Fig. 5). As shown in Fig. 5(a), the Fe_3O_4 cores are obviously surrounded by grey silica shells. The average size of the Fe_3O_4 cores and the support Fe_3O_4@SiO_2 are about 8–12 nm and 20 nm, respectively. As shown in Fig. 5(b), the size of **3** is about 20–30 nm. And after being reused six times, the morphology of recovered **3** does not show an obvious change (Fig. 5(c)).

The surface composition of **3** was analyzed with X-ray photoelectron spectroscopy (XPS). As shown in Fig. 6(a), the peaks with binding energy at 24.9, 102.2, 154.8, 284.9, 399.1, 531.7, 933.1 and 953.3 eV were assigned to O 2s, Si 2p, Si 2s, C 1s, N 1s, O 1s, Cu 2p$_{3/2}$ and Cu 2p$_{1/2}$, which affirmed that the catalyst was made up of C, O, Si, N and Cu. However, the peaks with binding energy at 711 and 723 eV were distributed to Fe 2p$_{3/2}$ and Fe 2p$_{1/2}$, which indicated that there is a little Fe_3O_4 present on the surface of catalyst **3**. The intense and broad peaks at 932.8 eV (Cu 2p$_{3/2}$) and 952.5 eV (Cu 2p$_{1/2}$) along with the presence of the characteristic shakeup satellite peaks suggest that the copper on the surface has an oxidation state of +2 (Fig. 6(b)).[82,83] Furthermore, in the N 1s spectrum of **3**, –N= (398.7 eV) and –NH– (399.5 eV) were observed (Fig. 6(c)).[84] In a word, it is clear that the secondary amine and Cu(II) were
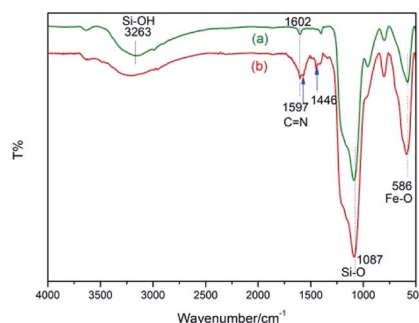

Scheme 1 Synthesis of MNP-supported bifunctional catalyst NH–Cu(II)@MNP (**3**). Reaction conditions: (a) toluene, N_2, reflux, 24 h; (b) pyridine-2-carbaldehyde, EtOH, N_2, reflux, 4 h; (c) $Cu(OAc)_2 \cdot H_2O$, acetone, N_2, RT, 24 h.

Fig. 3 FT-IR spectra of (a) Fe_3O_4@SiO_2 and (b) NH–Cu(II)@MNP.
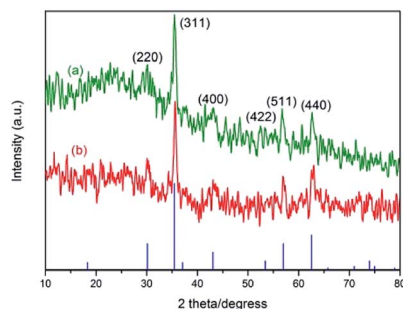
Fig. 4 XRD patterns of (a) $Fe_3O_4@SiO_2$ and (b) NH–Cu(II)@MNP catalyst **3**.

successfully anchored on the surface of the $Fe_3O_4@SiO_2$ support.

Besides, the elemental mapping images (see ESI†) also confirmed the existence of Fe, Si, N and Cu, and these elements species were equally distributed on the NH–Cu(II)@MNP. Furthermore, the distribution density of nitrogen and copper was less than that of iron and silicon. This was in accordance with the load ratio of copper and nitrogen on $Fe_3O_4@SiO_2$ support.

The thermostability of **3** was investigated by thermogravimetric analysis (Fig. 7). The TG curve indicates an initial weight loss of 1.3% up to 100 °C, which is ascribed to the adsorbed water. A main weight loss of 6.6% is observed from 350 to 620 °C, which is attributed to the decomposition of organic structure. The peak in the derivative thermogravimetric (DTG) curve shows that the fastest loss of the organic moiety occurred at 480 °C. Therefore, the thermostability of catalyst **3** is excellent.

The magnetic property was evaluated by vibrating sample magnetometer (VSM) test at room temperature (Fig. 8). The
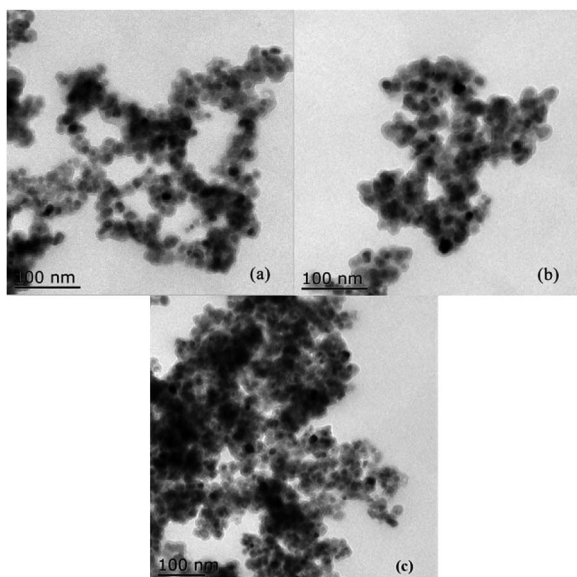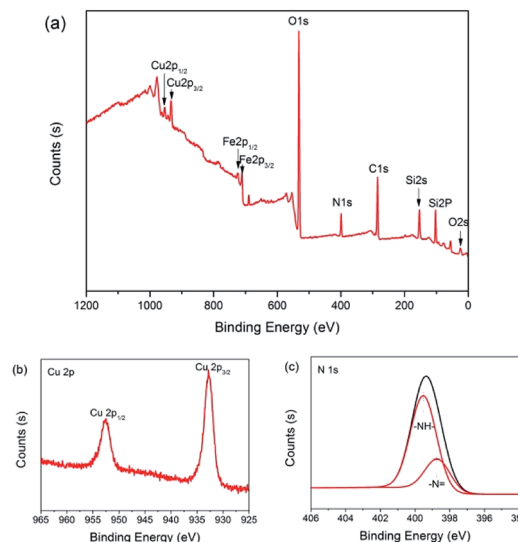

Fig. 6 The XPS spectra of the NH–Cu(II)@MNP catalyst **3**. (a) Survey scan; (b) Cu 2p and (c) N 1s.

magnetization of samples could be completely saturated at high fields of up to 1.5 T. And the maximum magnetic saturation intensity of **3** is 37.6 emu g^{-1} (Fig. 8(b)). The VSM magnetization curve of the sample goes through the zero point, so the catalyst has no magnetic hysteresis phenomenon, which indicates that the as-prepared catalyst is superparamagnetic.

The catalyst can be easily separated from the reaction system using an external magnet (Fig. 9).

The bifunctional catalytic performance of **3** was firstly investigated in a one-pot synthesis of (E)-3-phenyl-2-(1H-tetrazole-5-yl) acrylonitrile (**6a**) using benzaldehyde, malononitrile and sodium azide as the reactants. The domino reaction sequence was composed of two steps: Knoevenagel condensation and 1,3-dipolar cycloaddition. To clarify the bifunctional catalytic activity of **3**, the catalytic activities of a series of control samples were evaluated and the results are summarized in Table 1. For comparison, Cu(II)@MNP (**7**), NH∥Cu(II)@MNP (**8**, parallel immobilization of NH and Cu(II) on the same support like Fig. 1(b)) and N–Cu(II) (**9**) were also prepared (see ESI†).

The model Knoevenagel condensation of benzaldehyde (**4a**) and malononitrile at 80 °C was conducted using NH-L@MNP (**2**)
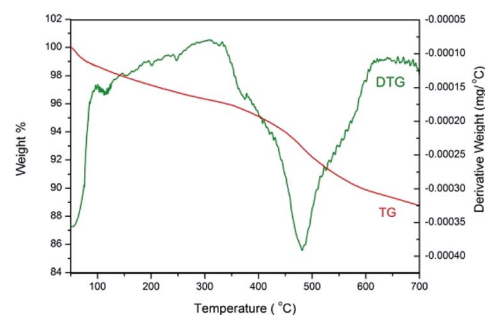

Fig. 5 TEM images of (a) $Fe_3O_4@SiO_2$, (b) NH–Cu(II)@MNP and (c) catalyst after being reused six times.

Fig. 7 Thermogravimetric (TG) and derivative thermogravimetric (DTG) curves for NH–Cu(II)@MNP.
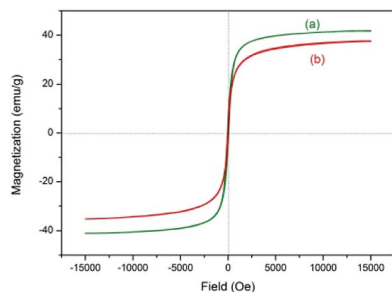
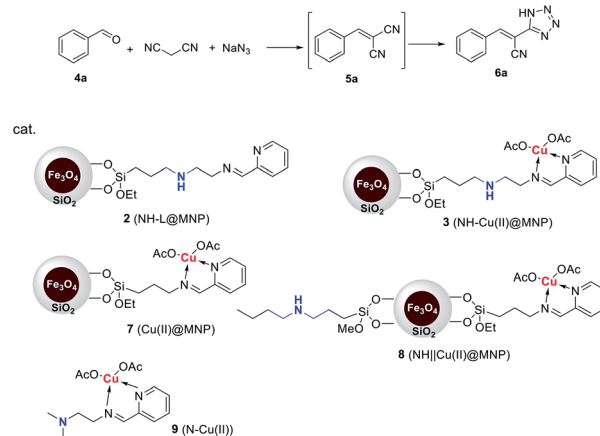**Fig. 8** VSM magnetization curve of (a) $Fe_3O_4@SiO_2$ and (b) $NH-Cu(II)$ @MNP.

and NH–Cu(II)@MNP (**3**) as catalysts. Both of them showed excellent activity while the latter was a little beat better (Table 1, entries 1–3). As for the control experiment without any catalyst, much longer time was required to get comparative yield (Table 1, entry 4). Meanwhile, the model 1,3-dipolar cycloaddition of **5a** and sodium azide catalyzed by **3** gave excellent yield (Table 1, entry 5). However, the control experiment using Cu(II)@MNP (**7**) as catalyst, longer reaction time was needed and lower yield was obtained (Table 1, entry 6). The domino reaction without any catalyst was conducted, both intermediate and final product were isolated but with low yields (Table 1, entry 7). Meanwhile, the support $Fe_3O_4@SiO_2$ and **2** had almost negligible effect on the yield of **6a** (Table 1, entries 8 and 9). But the product ratio (**6a** : **5a**) of the reaction changed. In the case of **7**, the desired product was obtained with a much higher yield of 69% (Table 1, entry 10). To our delight, the sequentially bifunctionalized catalyst **3** could efficiently catalyze the domino reaction and gave an excellent yield of 92% (Table 1, entry 11). In comparison, when a mixture of the two monofunctionalized catalysts **2** and **7** were used, only 72% of **6a** were obtained (Table 1, entry 12). Meanwhile, the parallelly bifunctionalized catalyst NH‖Cu(II)@MNP (**8**) afforded obviously lower yield (80%, Table 1, entry 13), which was in accordance with our hypothesis. That is, the sequentially bifunctionalized catalyst **3** exhibited superb catalytic activity and selectivity than parallelly bifunctionalized analogue, the reason must be that the relay catalytic process is in favor of the mass transfer of intermediate product. To explore the effect of support, the catalytic performance of a homogeneous catalyst N–Cu(II) (**9**) was tested, a significantly lower yield of 63% was obtained (Table 1, entry 15). The result showed that **9** displayed decreased catalytic efficiency. Moreover, we found

that the physical mixture of $Cu(OAc)_2$ and diethylamine exhibited lower catalytic activity too (Table 1, entry 14).

The domino reaction of benzaldehyde, malononitrile, sodium azide was investigated to find the optimal conditions (Table 2). The reaction without any catalyst afforded the product with low yield (Table 2, entry 1). Along with the increasing load of catalyst, the yield ascended accordingly (Table 2, entries 2 and 3). The best result was obtained by applying 20 mg of **3** as catalyst and conducting the reaction at 80 °C (Table 2, entry 4). More catalyst demonstrated no significant effect on the yield (Table 2, entries 6 and 7). Prolonging the reaction time to 10 h resulted in almost unchanged yield (Table 2, entry 5). Lower reaction temperature was unfavourable to the reaction (Table 2, entries 4, 8 and 9).

Thereafter, the above optimized reaction conditions were explored for the synthesis of a number of 5-substituted 1H-tetrazoles. As shown in Table 3, a variety of aldehydes reacted smoothly with malononitrile and sodium azide to afford the

Table 1 The catalytic activity of various catalysts[a]

Entry	Catalyst	T (°C)	t (h)	$5a^b$ (%)	$6a^b$ (%)
1^c	**2**	80	2.0	90	—
2^c	**3**	80	1.0	91	—
3^c	**3**	40	3.5	91	—
4^c	None	40	12.0	90	—
5^d	**3**	80	4.0	—	93
6^d	**7**	80	5.0	—	90
7	None	80	5.0	41	38
8	$Fe_3O_4@SiO_2$	80	5.0	35	43
9	**2**	80	5.0	26	50
10	**7**	80	5.0	17	69
11	**3**	80	5.0	5	92
12	**2 + 7**	80	5.0	15	72
13	**8**	80	5.0	13	80
14^e	$Cu(OAc)_2 + Et_2NH$	80	5.0	0	64
15^f	**9**	80	5.0	0	63

[a] Reaction conditions: benzaldehyde (1.0 mmol), malononitrile (1.1 mmol), sodium azide (1.2 mmol), catalyst (1 mol%, 20 mg), EtOH (10 mL), 80 °C. [b] Isolated yield. [c] Only for the Knoevenagel condensation of benzaldehyde and malononitrile, *i.e.* in the absence of sodium azide. [d] Only for the 1,3-dipolar cycloaddition of **5a** and sodium azide. [e] $Cu(OAc)_2$ (20 mol%), diethylamine (20 mol%). [f] N–Cu(II) (1 mol%).
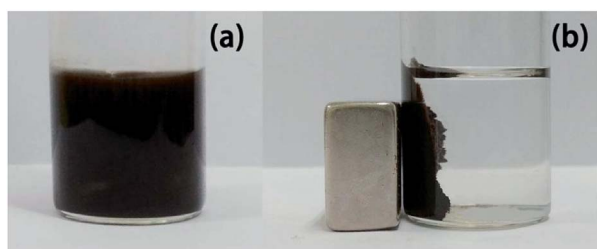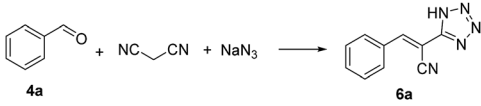

Fig. 9 A reaction mixture in the absence (a) or presence (b) of a magnetic field.

Table 2 Optimization of reaction conditions[a]

Entry	**3** (mg)	T (°C)	t (h)	Yield[b] (%)
1	0	80	5	39
2	5	80	5	66
3	15	80	5	90
4	20	80	5	92
5	20	80	10	91
6	50	80	5	91
7	100	80	5	89
8	20	50	5	75
9	20	20	5	13
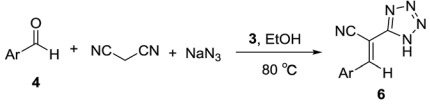
[a] Reaction conditions: benzaldehyde (1.0 mmol), malononitrile (1.1 mmol), sodium azide (1.2 mmol), NH–Cu(II)@MNP, EtOH (10 mL), 5 h. [b] **6a** (%), isolated yield.
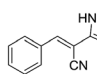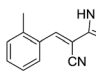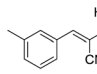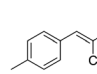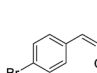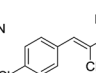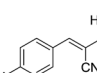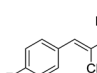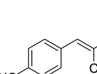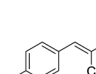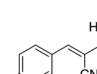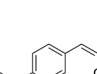
corresponding tetrazoles with excellent yields. *meta*-Methylbenzaldehyde (**4c**) resulted in a little higher yield than *ortho*-methylbenzaldehyde (**4b**) and *para*-methylbenzaldehyde (**4d**). The aldehydes containing electron-withdrawing groups like bromo, chloro, iodo, fluoro and cyano in *para* positions (**4e–i**) produced more satisfactory yields than those containing electron-donating groups like ethyl, isopropyl, methoxy and *tert*-butyl in *para* positions (**4j–m**). Heterocyclic aldehydes like

thiophene-2-carbaldehydes (**4n** and **4o**) also exhibited high reactivity and afforded the desired products with excellent yields. It is very strange that pyridine-2-carbaldehyde (**4p**) gave no desired product. When pyridine (1 equiv.) was added to the mixture of benzaldehyde, malononitrile, sodium azide and catalyst **3**, the yield of tetrazole was only 36%. Based on this result, we supposed that the coordination of pyridine moiety and copper prevented the formation of the target product. From the above results, it is obvious that **3** is an efficient catalyst for the preparation of large spectrum of substituted tetrazoles with very high yields in ethanol.
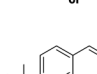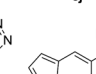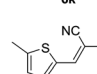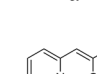
A plausible mechanism is shown in Scheme 2. Initially, the substrates were absorbed on the surface of the catalyst by hydrogen bonds. Then active α-H of malononitrile is abstracted by the secondary amine moiety (**A**) and the carbanion formed attacks the carbonyl, activated by acidic proton in ammonium, of benzaldehyde (**B**). After that, a synergistic dehydration occurs (**C**) to produce the intermediate product 2-benzylidenemalononitrile (**5a**). Subsequently, the coordination of the cyano group in 2-benzylidenemalononitrile with Cu(II) accompanying with anions exchange (replacement of acetate anion with azide) occurs (**D**), then a 1,3-dipolar cycloaddition between the C≡N group and azide anion takes place readily to form the tetrazole ring (**E**). Another anions exchange occurs to afford the catalyst and sodium tetrazolate, gives target product by acidic workup.

One of the most significant features of a catalyst is its recyclability. Thus, the recyclability of **3** were tested in the model reaction under the optimized reaction conditions. The catalyst was separated from the reaction mixture by an external magnet

Table 3 The NH–Cu(II)@MNP catalyzed one-pot synthesis of 5-substituted 1*H*-tetrazoles[a,b]

[a] Reaction conditions: aldehyde (1.0 mmol), malononitrile (1.1 mmol), sodium azide (1.2 mmol), catalyst **3** (20 mg), EtOH (10 mL), 80 °C. [b] Isolated yield.
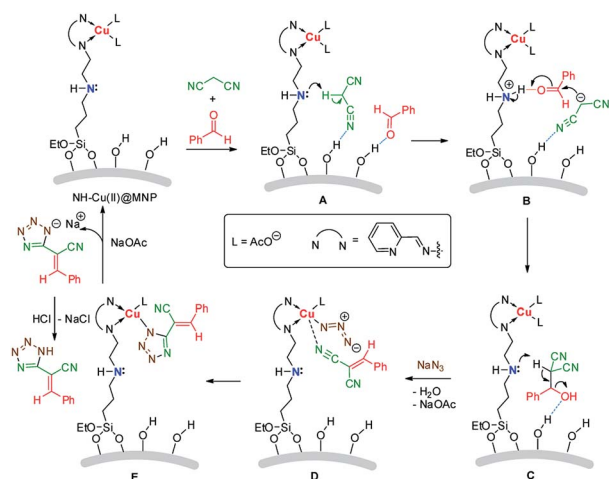
Scheme 2 Plausible reaction mechanism.
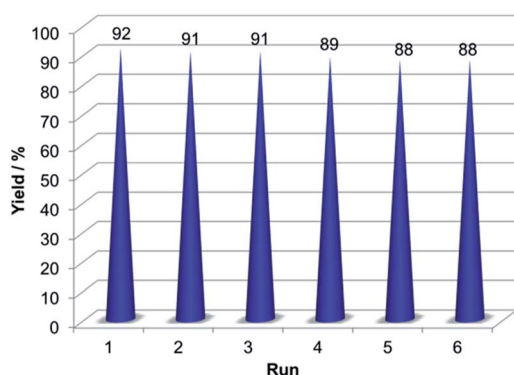
Fig. 10 Recycling experiment of the NH–Cu(II)@MNP.

and then washed with ethanol. Then the recovered catalyst was used in the next run. For all the six cycles, the catalyst could be reused without significant loss of catalytic activity (Fig. 10).

Conclusions

In summary, we have successfully established a relay catalysis strategy for one-pot domino reactions. A silica-coated nano-Fe_3O_4-supported bifunctional amine/Cu(II) catalyst was prepared and used in the synthesis of 5-substituted 1H-tetrazoles *via* a domino Knoevenagel condensation/1,3-dipolar cycloaddition pathway. Furthermore, the catalyst could be easily recovered from the reaction system by an external magnetic field and reused several times without loss of catalytic activity.

Experimental section

Materials

Toluene was dehydrated according to standard operation and stored on 4 Å molecular sieves. Other solvents and all of the reagents were commercially available and were used without

further purification. The core–shell $Fe_3O_4@SiO_2$ nanoparticles were prepared according to our previous work.[48]

Synthesis of NH@MNP (1)

$Fe_3O_4@SiO_2$ (1.0 g) was dispersed in anhydrous toluene (50 mL) by sonication for 1 h. [3-(2-Aminoethyl)aminopropyl]triethoxysilane (0.529 g, 2.0 mmol) was then added, and the reaction mixture was refluxed for 24 h under nitrogen atmosphere. After being cooled to room temperature, **1** was recycled by a permanent magnet, washed with dry toluene and acetone to remove unreacted species and then dried under vacuum overnight.

Synthesis of NH-L@MNP (2)

1 (1.0 g) was dispersed in anhydrous ethanol (40 mL) by sonication for 30 min. Pyridine-2-carbaldehyde (0.214 g, 2.0 mmol) was then added, and the resulting mixture was stirred under reflux for 4 h under nitrogen atmosphere. Product **2** was recycled by a permanent magnet, washed with extra dry ethanol and then dried under vacuum overnight.

Synthesis of NH–Cu(II)@MNP (3)

Copper sulfate monohydrate (0.399 g, 2.0 mmol) were dissolved in acetone (40 mL) and the solution was stirred at room temperature for 20 min, then **2** (1.0 g) was added. The final mixture was stirred at room temperature for 24 h under nitrogen atmosphere. The catalyst **3** was collected by a permanent magnet, washed several times with acetone and dried under vacuum overnight. The loading content of Cu was 1.3% as determined by inductively coupled plasma atomic emission spectroscopy (ICP-AES).

General procedure for the synthesis of tetrazoles 6

A mixture of aldehyde (1 mmol), malononitrile (1.1 mmol), sodium azide (1.2 mmol) and **3** (20 mg, 1.0 mol%) in EtOH (10 mL) was stirred at 80 °C for set time. After completion of the reaction, as indicated by TLC, the reaction mixture was cooled to ambient temperature. The catalyst **3** was recovered by the same procedure mentioned above and used for the next run. To the reaction mixture was added 2 N HCl (30 mL) under vigorous stirring to precipitate the product. Then the mother liquor was extracted by ethyl acetate (3 × 50 mL). The combined organic layers were dried over anhydrous Na_2SO_4 and evaporated under reduced pressure to obtain the crude product, the pure products were achieved by column chromatography on silica gel.

Conflicts of interest

There are no conflicts to declare.

Acknowledgements
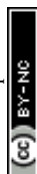
Notes and references

1 Y. Yang, X. Liu, X. Li, J. Zhao, S. Bai, J. Liu and Q. Yang, *Angew. Chem., Int. Ed.*, 2012, **51**, 9164–9168.

2 P. Li, C. Y. Cao, Z. Chen, H. Liu, Y. Yu and W. G. Song, *Chem. Commun.*, 2012, **48**, 10541–10543.

3 A. V. Biradar, V. S. Patil, P. Chandra, D. S. Doke and T. Asefa, *Chem. Commun.*, 2015, **51**, 8496–8499.

4 Y. Z. Chen, Y. X. Zhou, H. Wang, J. Lu, T. Uchida, Q. Xu, S. H. Yu and H. L. Jiang, *ACS Catal.*, 2015, **5**, 2062–2069.

5 L. C. Lee, J. Lu, M. Weck and C. W. Jones, *ACS Catal.*, 2016, **6**, 784–787.

6 Z. Jia, K. Wang, B. Tan and Y. Gu, *ACS Catal.*, 2017, **7**, 3693–3702.

7 U. Diaz, D. Brunel and A. Corma, *Chem. Soc. Rev.*, 2013, **42**, 4083–4097.

8 P. Zhao, Y. Zhang, Y. Wang, H. Cui, F. Song, X. Sun and L. Zhang, *Green Chem.*, 2018, **20**, 1551–1559.

9 P. Li, Y. Yu, H. Liu, C. Y. Cao and W. G. Song, *Nanoscale*, 2014, **6**, 442–448.

10 Z. Miao, Y. Luan, C. Qi and D. Ramella, *Dalton Trans.*, 2016, **45**, 13917–13924.

11 H. Wang, Y. Wang, Y. Guo, X. K. Ren, L. Wu, L. Liu, Z. Shi and Y. Wang, *Catal. Today*, 2019, **330**, 124–134.

12 B. Lai, F. Mei and Y. Gu, *Chem.–Asian J.*, 2018, **13**, 2529–2542.

13 B. Voit, *Angew. Chem., Int. Ed.*, 2006, **45**, 4238–4240.

14 K. Motokura, N. Fujita, K. Mori, T. Mizugaki, K. Ebitani and K. Kaneda, *J. Am. Chem. Soc.*, 2005, **127**, 9674–9675.

15 R. K. Zeidan, S. J. Hwang and M. E. Davis, *Angew. Chem., Int. Ed.*, 2006, **45**, 6332–6335.

16 S. Shylesh, A. Wagener, A. Seifert, S. Ernst and W. R. Thiel, *Angew. Chem., Int. Ed.*, 2010, **49**, 184–187.

17 N. R. Shiju, A. H. Alberts, S. Khalid, D. R. Brown and G. Rothenberg, *Angew. Chem., Int. Ed.*, 2011, **50**, 9615–9619.

18 K. Motokura, M. Tada and Y. Iwasawa, *J. Am. Chem. Soc.*, 2009, **131**, 7944–7945.

19 F. Shang, J. Sun, H. Liu, C. Wang, J. Guan and Q. Kan, *Mater. Res. Bull.*, 2012, **47**, 801–806.

20 F. Shang, J. Sun, S. Wu, Y. Yang, Q. Kan and J. Guan, *Microporous Mesoporous Mater.*, 2010, **134**, 44–50.

21 E. Merino, E. Verde-Sesto, E. M. Maya, M. Iglesias, F. Sánchez and A. Corma, *Chem. Mater.*, 2013, **25**, 981–988.

22 Y. Zhang, B. Li and S. Ma, *Chem. Commun.*, 2014, **50**, 8507–8510.

23 B. Li, Y. Zhang, D. Ma, L. Li, G. Li, G. Li, Z. Shi and S. Feng, *Chem. Commun.*, 2012, **48**, 6151–6153.

24 F. Zhang, H. Jiang, X. Li, X. Wu and H. Li, *ACS Catal.*, 2014, **4**, 394–401.

25 F. Zhang, H. Jiang, X. Wu, Z. Mao and H. Li, *ACS Appl. Mater. Interfaces*, 2015, **7**, 1669–1677.

26 S. Shylesh, A. Wagner, A. Seifert, S. Ernst and W. R. Thiel, *Chem.–Eur. J.*, 2009, **15**, 7052–7062.

27 J. Gao, X. Zhang, Y. Lu, S. Liu and J. Liu, *Chem.–Eur. J.*, 2015, **21**, 7403–7407.

28 Y. Huang, S. Xu and V. S. Lin, *Angew. Chem., Int. Ed.*, 2011, **50**, 661–664.

29 L. Liu, Y. Ai, D. Li, L. Qi, J. Zhou, Z. Tang, Z. Shao, Q. Liang and H. B. Sun, *ChemCatChem*, 2017, **9**, 3131–3137.

30 Z. Weng, T. Yu and F. Zaera, *ACS Catal.*, 2018, **8**, 2870–2879.

31 R. Kardooni and A. R. Kiasat, *J. Taiwan Inst. Chem. Eng.*, 2018, **87**, 241–251.

32 P. Chandra, A. M. Jonas and A. E. Fernandes, *ACS Catal.*, 2018, **8**, 6006–6011.

33 L. Xiong, H. Zhang, Z. He, T. Wang, Y. Xu, M. Zhou and K. Huang, *New J. Chem.*, 2018, **42**, 1368–1372.

34 S. Shylesh, V. Schunemann and W. R. Thiel, *Angew. Chem., Int. Ed.*, 2010, **49**, 3428–3459.

35 S. Yang, C. Cao, Y. Sun, P. Huang, F. Wei and W. Song, *Angew. Chem., Int. Ed.*, 2015, **54**, 2661–2664.

36 Z. S. Wu, S. Yang, Y. Sun, K. Parvez, X. Feng and K. Mullen, *J. Am. Chem. Soc.*, 2012, **134**, 9082–9085.

37 J. Dai, H. Zou, R. Wang, Y. Wang, Z. Shi and S. Qiu, *Green Chem.*, 2017, **19**, 1336–1344.

38 A. Mohammadinezhad and B. Akhlaghinia, *Green Chem.*, 2017, **19**, 5625–5641.

39 W. Gu, X. Deng, X. Jia, J. Li and E. Wang, *J. Mater. Chem. A*, 2015, **3**, 8793–8799.

40 R. B. Baig and R. S. Varma, *Chem. Commun.*, 2013, **49**, 752–770.

41 Q. Deng, Y. Shen, H. Zhu and T. Tu, *Chem. Commun.*, 2017, **53**, 13063–13066.

42 V. Polshettiwar, R. Luque, A. Fihri, H. Zhu, M. Bouhrara and J. M. Basset, *Chem. Rev.*, 2011, **111**, 3036–3075.

43 M. J. Jin and D. H. Lee, *Angew. Chem., Int. Ed.*, 2010, **49**, 1119–1122.

44 Q. Yue, J. Li, Y. Zhang, X. Cheng, X. Chen, P. Pan, J. Su, A. A. Elzatahry, A. Alghamdi, Y. Deng and D. Zhao, *J. Am. Chem. Soc.*, 2017, **139**, 15486–15493.

45 I. Elsayed, M. Mashaly, F. Eltaweel, M. A. Jackson and E. B. Hassan, *Fuel*, 2018, **221**, 407–416.

46 N. Azgomi and M. Mokhtary, *J. Mol. Catal. A: Chem.*, 2015, **398**, 58–64.

47 R. Gupta, M. Yadav, R. Gaur, G. Arora and R. K. Sharma, *Green Chem.*, 2017, **19**, 3801–3812.

48 Q. Zhang, H. Su, J. Luo and Y. Wei, *Green Chem.*, 2012, **14**, 201–208.

49 Q. Zhang, H. Su, J. Luo and Y. Wei, *Catal. Sci. Technol.*, 2013, **3**, 235–243.

50 S. Wang, Z. Zhang, B. Liu and J. Li, *Catal. Sci. Technol.*, 2013, **3**, 2104–2112.

51 N. Mir, A. Heidari, H. Beyzaei, S. Mirkazehi-Rigi and P. Karimi, *Chem. Eng. J.*, 2017, **327**, 648–655.

52 Q. Zhou, Z. Wan, X. Yuan and J. Luo, *Appl. Organomet. Chem.*, 2016, **30**, 215–220.

53 S. Wang, J. Tang, H. Zhao, J. Wan and K. Chen, *J. Colloid Interface Sci.*, 2014, **432**, 43–46.

54 J. Zhou, Y. Li, H.-b. Sun, Z. Tang, L. Qi, L. Liu, Y. Ai, S. Li, Z. Shao and Q. Liang, *Green Chem.*, 2017, **19**, 3400–3407.

55 Y. Ai, Z. Hu, Z. Shao, L. Qi, L. Liu, J. Zhou, H. Sun and Q. Liang, *Nano Res.*, 2018, **11**, 287–299.

56 T. Zeng, L. Yang, R. Hudson, G. Song, A. R. Moores and C. J. Li, *Org. Lett.*, 2011, **13**, 442–445.
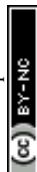
57 V. Rama, K. Kanagaraj and K. Pitchumani, *J. Org. Chem.*, 2011, **76**, 9090–9095.

58 M. Zarghani and B. Akhlaghinia, *RSC Adv.*, 2016, **6**, 31850–31860.

59 M. Massi, S. Stagni and M. I. Ogden, *Coord. Chem. Rev.*, 2018, **375**, 164–172.

60 T. A. Kuz'menko, A. S. Morkovnik, L. N. Divaeva, G. S. Borodkin and V. V. Kuz'menko, *Chem. Heterocycl. Compd.*, 2015, **50**, 1575–1585.

61 D. C. Zhong, Y. Q. Wen, J. H. Deng, X. Z. Luo, Y. N. Gong and T. B. Lu, *Angew. Chem., Int. Ed.*, 2015, **54**, 11795–11799.

62 S. Khaghaninejad, M. M. Heravi, T. Hosseinnejad, H. A. Oskooie and M. Bakavoli, *Res. Chem. Intermed.*, 2016, **42**, 1593–1610.

63 R. P. Singh, R. D. Verma, D. T. Meshri and J. M. Shreeve, *Angew. Chem., Int. Ed.*, 2006, **45**, 3584–3601.

64 A. L. Chandgude and A. Domling, *Green Chem.*, 2016, **18**, 3718–3721.

65 Z. N. Tisseh, M. Dabiri, M. Nobahar, H. R. Khavasi and A. Bazgir, *Tetrahedron*, 2012, **68**, 1769–1773.

66 F. Himo, Z. P. Demko, L. Noodleman and K. B. Sharpless, *J. Am. Chem. Soc.*, 2002, **124**, 12210–12216.

67 F. Himo, Z. P. Demko, L. Noodleman and K. B. Sharpless, *J. Am. Chem. Soc.*, 2003, **125**, 9983–9987.

68 D. Habibi, M. Nasrollahzadeh and Y. Bayat, *Synth. Commun.*, 2011, **41**, 2135–2145.

69 S. Kumar, S. Dubey, N. Saxena and S. K. Awasthi, *Tetrahedron Lett.*, 2014, **55**, 6034–6038.

70 D. Kong, Y. Liu, J. Zhang, H. Li, X. Wang, G. Liu, B. Li and Z. Xu, *New J. Chem.*, 2014, **38**, 3078–3083.

71 D. R. Patil, Y. B. Wagh, P. G. Ingole, K. Singh and D. S. Dalal, *New J. Chem.*, 2013, **37**, 3261–3266.

72 P. Mani, A. K. Singh and S. K. Awasthi, *Tetrahedron Lett.*, 2014, **55**, 1879–1882.

73 F. Dehghani, A. R. Sardarian and M. Esmaeilpour, *J. Organomet. Chem.*, 2013, **743**, 87–96.

74 M. Abdollahi-Alibeik and A. Moaddeli, *New J. Chem.*, 2015, **39**, 2116–2122.

75 M. Esmaeilpour, J. Javidi and S. Zahmatkesh, *Appl. Organomet. Chem.*, 2016, **30**, 897–904.

76 M. Esmaeilpour, J. Javidi, F. Nowroozi Dodeji and M. Mokhtari Abarghoui, *J. Mol. Catal. A: Chem.*, 2014, **393**, 18–29.

77 M. Khanmoradi, M. Nikoorazm and A. Ghorbani-Choghamarani, *Appl. Organomet. Chem.*, 2017, **31**, e3693.

78 M. Abdollahi-Alibeik and A. Moaddeli, *J. Chem. Sci.*, 2016, **128**, 93–99.

79 F. Taghavi, M. Gholizadeh, A. S. Saljooghi and M. Ramezani, *MedChemComm*, 2017, **8**, 1953–1964.

80 A. Ghorbani-Choghamarani, L. Shiri and G. Azadi, *RSC Adv.*, 2016, **6**, 32653–32660.

81 G. Azadi, A. Ghorbani-Choghamarani and L. Shiri, *Transition Met. Chem.*, 2017, **42**, 131–136.

82 L. Liao, Y. Liu, Z. Li, J. Zhuang, Y. Zhou and S. Chen, *RSC Adv.*, 2016, **6**, 94976–94988.

83 L. Chen, B. Li and D. Liu, *Catal. Lett.*, 2014, **144**, 1053–1061.

84 B. Huang, Y. Liu, B. Li, S. Liu, G. Zeng, Z. Zeng, X. Wang, Q. Ning, B. Zheng and C. Yang, *Carbohydr. Polym.*, 2017, **157**, 576–585.